Wood Chemistry

Shori Imamura, Masaki Hosokawa, Yasuyuki Matsushita*, Dan Aoki, Kazuhiko Fukushima and Masato Katahira

Quantitative analysis of the β-1 structure in lignin by administration of [ring-1-¹³C]coniferin

https://doi.org/10.1515/hf-2023-0100 Received October 5, 2023; accepted December 19, 2023; published online January 4, 2024

Abstract: Lignin dimeric units are characterized by various inter-unit linkage types such as β -O-4, β -5, β - β , and β -1. Spirodienones are the native form of the β -1 structures, but the content in lignin has not been clarified. In this study, the ring-1-13C labeled coniferin was synthesized and administered to Ginkgo biloba shoots, obtaining ring-1 selectively labeled xylem samples. Enzymatically saccharified lignin (EL) samples were prepared from the xylem sample (400-600 µm distant region from the cambial zone), and solutionstate quantitative 13C NMR and solid-state CP/MAS NMR measurements were conducted. Acetylated EL (ELAc) was also prepared from the xylem sample (600–800 µm distant region from the cambial zone), and solution-state quantitative ¹³C NMR and ¹H-¹³C 2D NMR measurements were conducted. Difference spectra obtained by subtracting the unlabeled spectra from the ring-1 labeled spectra showed that the ring-1 was responsible for broad signals at 134 ppm and signals of the spirodienone structure at 56.11 ppm (in solid-state), 54.70 ppm (EL in solution-state), and 54.72 ppm (ELAc in solution-state). The ratio of spirodienone structure was evaluated as 0.68 % (EL) and 0.72 % (ELAc) by the solution-state quantitative ¹³C difference spectra, and 2.3 % (ELAc) by HSQC volume ratio of Cα'-H to G2-H.

Keywords: isotope labeling; precursor administration; quantitative NMR; solid-state NMR; spirodienone

1 Introduction

Lignin is one of the main components of cell walls and is a macromolecule that provides hydraulic conductivity, antibacterial properties, and strength. Lignin is formed by radical coupling polymerization of monolignols such as coniferyl alcohol, sinapyl alcohol, and p-coumaryl alcohol. As monolignol radicals are electron-delocalized, many types of bonds occur between monolignols, including β -O-4, β -5, β - β , and β -1, resulting in lignin being a highly complex three-dimensional polymer.

Lignin is the second most abundant organic plant polymer and is attracting attention as an alternative to fossil resources. It is essential to understand its structure well to overcome the difficulty of structural complexity and effectively use lignin. In particular, the β-1 linkage, which is the bond between C1 of the aromatic ring (ring-1) of the lignin phenol terminal group and Cβ of the monolignol, is one of the most important bonds for the chemical reaction of lignin, although it is a minor linkage, because it has a highly reactive dienone structure. Chemical degradation methods release 1,2-diaryl propane-1,3-diol type structures (Lundquist and Mikshe 1965; Lundquist 1987; Matsumoto et al. 1984). Recently, as a non-destructive method, nuclear magnetic resonance spectroscopy (NMR) has been performed to analyze lignin's detailed chemical structure. However, such structures are trace amounts and not quantifiable by NMR (Ede et al. 1996; Habu et al. 1990).

The 2D NMR and the experience approach using model compounds reveals that the β -1 linkage can form a spirodienone-type structure (Ämmälahti et al. 1998; Brunow et al. 1998; Capanema et al. 2005; del Río et al. 2009, 2011; Ralph et al. 2004; Rencoret et al. 2008, 2011; Setälä et al. 1999; Zhang et al. 2006; Zhang and Gellerstedt 2001). Ralph et al. (2019) concluded that the β -1 linkage in plant lignin exists mainly in the spirodienone-type structure and rarely in the 1,2-diarylpropane-1,3-diol-type structure (Figure 1). Spirodienone-type structures are readily converted to the 1,2-diarylpropane-1,3-diol-type structure through specific chemical treatments under acidic conditions.

^{*}Corresponding author: Yasuyuki Matsushita, Institute of Agriculture, Tokyo University of Agriculture and Technology, Tokyo 183-8509, Japan, E-mail: yasu@go.tuat.ac.jp. https://orcid.org/0000-0003-1357-3927

Shori Imamura, Masaki Hosokawa, Dan Aoki and Kazuhiko

Fukushima, Graduate School of Bioagricultural Sciences, Nagoya

University, Nagoya, Japan. https://orcid.org/0000-0003-3696-4103 (D. Aoki)

Masato Katahira, Institute of Advanced Energy, Kyoto University, Kyoto, Japan

Figure 1: Structures of β-1 linkage in lignin.

Obtaining quantitative information about the spirodienone-type structure is important for modifying lignin into functional materials; however, its minor content in lignin makes it difficult. It has been reported that the abundance of this linkage ranges from <3 % (Ede et al. 1990) to about 10 % (Higuchi 1990). In this study, [ring-1- 13 C]coniferin was synthesized and administered to *Gingko biloba* L. The spirodienone structure content in the lignin was estimated using 13 C-labeling techniques and 13 C NMR analysis.

2 Materials and methods

2.1 Synthesis of [ring-1-13C]coniferin

The schematic synthesis of [ring-1-13C] coniferin is shown in Figure 2.

2.2 Synthesis of [ring-1-¹³C] ethyl 4-hydroxybenzoate

In a round-bottomed flask, [2–¹³C]diethyl malonate (1 g, 6.25 mmol) and 1 equivalent of 4*H*-pyran-4-one (0.6 g, 6.25 mmol) were dissolved in tertbutyl alcohol (8 mL), and the flask was purged with Argon gas. A cooling tube with a calcium tube and an isobaric dripping funnel containing potassium-tert-butoxide (0.7 g, 6.25 mmol) dissolved in tert-butyl alcohol (13 mL) was attached to a three-necked round-bottom flask, and the mixture was heated at 115 °C. After the start of refluxing, a potassium-tert-butoxide solution was added dropwise over 0.5 h with stirring. The reaction was kept for 2.5 h, and then 13 mL of 1 M HCl was added dropwise. The reaction temperature was reset to 105 °C, and reflux was continued for 1 h. After cooling, the reaction product was extracted with ethyl acetate. The organic layer was washed with distilled water, saturated brine and dried with anhydrous sodium sulfate. The extract was concentrated under reduced pressure to remove the solvent, and the crude [ring-1-¹³C] ethyl 4-hydroxybenzoate (1.1 g, crude yield 105 %) was

Figure 2: Synthesis of [ring-1-¹³C]coniferin. Yield is shown in parentheses. *Crude yield.

obtained. ¹H NMR (in CDCl₃) δ : 1.38 (3H, t, I = 7.1 Hz), 4.35 (2H, q, 7.1 Hz), 6.90 (2H, m), 7.94 (2H d, 8.3 Hz). ¹³C-NMR δ : 14.41, 61.10, 115.39, 122.32, 131.98, 160.82, 167.32. The $^1\mathrm{H}$ and $^{13}\mathrm{C}$ NMR spectra are shown in Figure S1.

2.3 Synthesis of [ring-1-13C] 4-hydroxy benzyl alcohol

LiAlH₄ (400 mg) and 20 mL of anhydrous diethyl ether were mixed in a round-bottom flask under nitrogen gas. All of the crude product of [ring-1-13C] ethyl 4-hydroxybenzoate synthesized was dissolved in anhydrous diethyl ether (20 mL) and added dropwise to the flask with stirring for 1.5 h under a nitrogen atmosphere. The reaction was allowed to proceed for 3 h. The reaction solution was cooled to 0 °C and quenched by slowly adding a mixture of diethyl ether: ethanol = 9:1 (20 mL). It was acidified with dry ice, and the mixture was extracted with ethyl acetate. After drying using anhydrous sodium sulfate, the solvent was removed under reduced pressure to obtain the crude [ring-1-13C] 4-hvdroxy benzyl alcohol (0.46 g, crude yield 56 %). ¹H NMR (in acetone- d_6) δ : 4.51 (2H, m), 6.78 (2H, dd, 8.6, J = 7.2 Hz), 7.18 (2H, d, J = 8.6 Hz). ¹³C-NMR δ : 64.55, 115.74, 129.05, 134.16, 157.25. The ¹H and ¹³C NMR spectra are shown in Figure S2.

2.4 Synthesis of [ring-1-¹³C] 4-hydroxybenzaldehyde

To a round-bottomed flask was added the crude [ring-1-13C] 4-hydroxy benzyl alcohol (0.46 g) and dicyclohexylamine (0.67 g), which was dissolved in THF (3 mL). RuCl3 (25 mg) was added to the flask, and the reaction was kept at room temperature with stirring until the substrate diminished, with the addition of RuCl₃ (25 mg) as needed. The reaction mixture was acidified with 1 M HCl and extracted with ethyl acetate. The organic layer was washed with distilled water and then with saturated brine. The extract was subjected to filtration and a silica gel short column to remove RuCl₃ and dried with anhydrous sodium sulfate. After removing the solvent under reduced pressure, chloroform was added to the dried solid. The insoluble material was removed by filtrate. The organic solution was concentrated under reduced pressure to obtain the crude [ring-1-13C] 4-hydroxybenzaldehyde (0.34 g, crude yield 75 %). ¹H NMR (in acetone- d_6) δ : 7.02 (2H, m), 7.81 (2H, m), 9.86 (1H, d, J = 24.0 Hz). ¹³C-NMR δ: 116.67, 130.50, 132.82, 163.87, 191.00. The ¹H and ¹³C NMR spectra are shown in Figure S3.

2.5 Synthesis of [ring-1-13C]3-bromo-4-hydroxybenzaldehyde

To a round-bottomed flask was added the crude [ring-1-13C] 4-hydro xybenzaldehyde (0.34 g) dissolved in chloroform (25 mL) at 0 °C, and a chloroform solution of bromine (0.43 g, in 20 mL) was added dropwise over 0.5 h with stirring. The reaction was kept overnight at room temperature. The reaction solution was washed with distilled water and dried with anhydrous sodium sulfate. The organic layer was concentrated under reduced pressure to obtain crude [ring-1-13C] 3-bromo-4-hydroxybenzaldehyde (0.47 g, crude yield 84 %). ¹H NMR (in acetone- d_6) δ : 7.20 (1H, t, J = 8.1 Hz), 7.80 (1H, dd, 8.36, J = 1.92 Hz), 8.07 (1H, d, J = 1.8 Hz), 9.86 (1H, d, J = 25.0 Hz). ¹³C-NMR δ : 110.99, 117.40, 131.69, 132.32, 135.44, 160.19, 190.17. The ¹H and ¹³C NMR spectra are shown in Figure S4.

2.6 Synthesis of Iring-1-13 Clyanillin

In a round-bottomed flask, the crude [ring-1-13C] 3-bromo-4-hydro xybenzaldehyde (0.45 g) and copper (II) chloride (0.18 g) as a catalyst were dissolved in 1-methylimidazole (3.75 mL). A sodium (0.34 g) solution dissolved in 10 mL of dehydrated methanol was added to the flask and set in an oil bath. The oil bath was set to 130 °C and heated while nitrogen gas flowed to evaporate and remove the methanol. It was refluxed for 1 h under a nitrogen atmosphere. The flask was cooled in ice water, and the reaction mixture was acidified with 1 M HCl. The solution was extracted with ethyl acetate, washed with water and saturated brine, and dried with anhydrous sodium sulfate. The organic layer was concentrated under reduced pressure. The crude product was purified by silica gel column chromatography (ethyl acetate: hexane = 1:3) to obtain [ring-1- 13 C]vanillin (vield 46 %). 1 H NMR (in acetone- d_6) δ : 3.94 (3H. s), 7.02 (1H, m), 7.45 (1H, d, I = 1.84 Hz), 7.48 (1H, m), 9.83 (1H, d, I = 24.4 Hz); ¹³C-NMR δ: 56.30, 110.89, 115.94, 126.95, 130.74, 148.97, 153.55, 191.07. The ¹H and ¹³C NMR spectra are shown in Figure S5.

2.7 Synthesis of [ring-1-13C]tetra-O-acetylglucovanillin

To a two-necked pear-shaped flask was added [ring-1-13C] vanillin (0.5 g, 3.3 mmol) and 2,3,4,6-O-acetyl-α-p-bromoglucose (1.35 g, 3.3 mmol), dissolved in 4 mL of quinoline and the flask was placed in ice water to cool. Silver oxide (I) (0.38 g, 1.65 mmol) was added to the mixture and allowed to react for 1.5 h under stirring. After adding acetic acid (4 mL), the reaction solution was added to cold water and stirred. It was run through a layer of celite on filter paper and filtered by suction. The precipitate remaining on the Celite layer was collected and extracted with hot ethanol. From the ethanol solution, [ring-1-13C] tetra-O-acetylglucovanillin was obtained by recrystallization (yield 78 %). ¹H NMR (in acetone- d_6) δ : 1.98 (3H, s), 2.02 (3H, s), 2.03 (3H, s), 2.03 (3H, s), 3.91 (3H, s), 4.23 (1H, m), 4.30 (1H, m), 5.15 (1H, m), 5.26 (1H, m) 5.40 (1H, m), 5.50 (1H, m), 7.40 (1H, m), 7.51 (1H, m), 7.54 (1H, dd, I = 8.2 Hz, 1.84 Hz), 9.92 (1H, d, I =24.7 Hz); ¹³C-NMR δ: 20.54, 20.57, 20.60, 20.62, 56.55, 62.68, 69.22, 71.84, 72.84, 73.17, 99.83, 112.13, 118.17, 125.40, 133.68, 151.61, 152.23, 169.61, 170.04, 170.31, 170.65, 191.53. The 1 H and 13 C NMR spectra are shown in Figure S6.

2.8 Synthesis of [ring-1-13C]ethyl tetra-0acetylglucoferulate

To an 18 mm diameter screw-capped test tube was added the synthesized [ring-1-13C]tetra-O-glucovanillin (1.22 g, 2.5 mmol) and monoethyl malonate (0.34 g, 2.6 mmol) dissolved in 1.0 mL of pyridine. A few drops of piperidine were added to the test tube, and the reaction was carried out in an oil bath at 100 °C for 1.5 h. The reaction solution was transferred to cooled distilled water and neutralized with dilute hydrochloric acid. It was run through a celite layer on filter paper, filtered by suction, and washed with distilled water. The precipitate remaining on the celite layer was collected and extracted with hot ethanol, and [ring-1-13C]ethyl tetra-O-acetylglucoferulate was obtained from the ethanol solution by recrystallization (yield 87 %). ¹H NMR (in acetone- d_6) δ : 1.28 (3H, t, J = 7.1 Hz), 1.98 (3H, s), 2.02 (3H, s), 2.03 (6H, s), 3.90 (3H, s), 4.17 (1H, m), 4.21 (1H, m), 4.29 (1H, m), 5.13 (1H, m), 5.22 (1H, m), 5.38 (1H, m), 5.53 (1H, m), 6.49 (1H, dd, I = 16.2 Hz, 2.1 Hz), 7.23 (1H, m), 7.25 (1H, s), 7.40 (1H, s), 7.61

(1H, dd, 16.0 Hz, 2.04 Hz); $^{13}\text{C-NMR}$ 8: 14.63, 20.54, 20.60, 20.64, 56.58, 60.70, 62.43, 69.32, 71.94, 72.71, 73.24, 100.40, 112.55, 118.23, 119.24, 122.70, 131.49, 144.73, 149.06, 151.55, 167.16, 169.64, 170.05, 170.31, 170.66. The ^1H and ^{13}C NMR spectra are shown in Figure S7.

2.9 Synthesis of [ring-1-13C]coniferin

[ring-1-13C]Ethyl tetra-O-acetylglucoferulate (1.26 g, 2.6 mmol) and anhydrous toluene (40 mL) were added to a four-necked round-bottom flask. DIBAL-H (21.2 mL, 31.8 mmol) was added dropwise to the flask over 0.5 h under a nitrogen atmosphere at 0 °C and allowed to react for 1 h. Anhydrous ethanol (10 mL) was added to guench the reducing agent, and the reaction solution was concentrated under reduced pressure. Toluene was removed by adding distilled water and further concentrating under reduced pressure, and the resulting solid was extracted with hot water. From the water solution, [ring-1-13C]coniferin was obtained by recrystallization (yield 58 %). 1H NMR (in acetone- d_6) δ : 3.14–3.31 (4H), 3.45 (1H, m), 3.66 (1H, m), 3.78 (3H, s), 4.10 (2H, m), 4.53 (1H, t, J = 5.7 Hz), 4.82 (1H, t, J = 5.5 Hz), 4.89 (1H, d, J = 5.5 Hz)7.16 Hz), 5.00 (1H, d, J = 5.2 Hz), 5.07 (1H, d, J = 4.2 Hz), 5.22 (1H, d, J = 4.9 Hz), 6.28 (1H, m), 6.47 (1H, d, J = 14.9 Hz), 6.89 (1H, d, J = 8.4 Hz), 7.01 Hz(1H, d, J = 8.4 Hz), 7.05 (1H, s); ¹³C-NMR δ : 55.63, 60.66, 61.65, 69.67, 73.21, 76.84, 77.04, 100.00, 109.55, 115.25, 119.31, 128.12, 129.00, 131.00, 146.04, 149.08. The ¹H and ¹³C NMR spectra are shown in Figure S8.

2.10 Administration of [ring-1-¹³C]coniferin to *G. biloba* shoots

According to a previously described method (Aoki et al. 2019; Terashima et al. 2002, 2003), [ring-1- 13 C]coniferin was administrated to *G. biloba* shoots to enrich 13 C at the ring-1 position of the lignin specifically. The administration began in mid-June 2018. Cut ginkgo shoots (3 years old, 20–25 cm in axial length) were placed into small vials containing a 4 % aqueous solution of either [ring-1- 13 C]coniferin or coniferin in a growth chamber under 12 h at 24 °C: 12 h at 20 °C as the light: dark period. For the no administration group, tap water was given instead of the coniferin solutions. A total of 9 ginkgo shoots were grown: 3 for 13 C labeling (L-1, 2, 3), 3 for non-labeling (NL-1, 2, 3), and 3 for no administration (Ctrl-1, 2, 3). When the total dosage reached 300 mg, the plants were grown in tap water for about one month.

The grown ginkgo shoots were pruned off the branches and leaves, and the bark was peeled with a knife. The newly formed xylem was peeled from the shoots with a peeler and stored in 50 % ethanol. The layer thickness was approximately 200 μm . The peeling was repeated five times to obtain samples having different distances from the cambial zone of 0–200 μm , 200–400 μm , 400–600 μm , 600–800 μm , and 800–1000 μm . Next, each layer was extracted with acetone for 8 h by Soxhlet extraction, then extracted with hot water at 80 °C for 8 h. After extraction, the newly formed xylem was freeze-dried and subjected to a cutting mill (PULVERISETTE 14 classic line, FRITSCH GmbH, Idar-Oberstein, Germany).

2.11 Determination of ¹³C labeling ratio of samples

Thioacidolysis was performed according to previous methods (Lapierre et al. 1985, 1986; Shimizu et al. 2021). The ¹³C labeling ratio of samples was determined by GC-MS analysis of thioacidolysis degradation products. Similar calculations were previously described in detail (Miyata et al. 2023).

The lignocellulosic sample and n-docosane as internal standard were added into a 15 mL screw-cap reaction vial and treated with thioacidolysis reagent (10 mL; a mixture of ethanethiol (50 mL), boron trifluoride diethyl ether complex (12.5 mL) and dioxane (37.5 mL)) at 100 °C for 4 h. The vial was then cooled with water, and 0.4 M sodium hydrogen carbonate (2 mL) was added. The reaction mixture was acidified with hydrochloric acid and extracted with dichloromethane. After drying with sodium sulfate, the organic layer was concentrated to ca. 1.5 mL. The solution was subjected to GC-MS analysis (Shimadzu GCMS-QP 2010) after trimethylsilylation with N,O-bis(trimethylsilyl)trifluoroacetamide. The analysis conditions were as follows: column temperature was programmed as follows: 2.0 °C/min from 180 °C to 230 °C, 15.0 °C/min from 230 °C to 300 °C, and then 300 °C for 10 min.

The relative frequency of m/z 269–277 (exp-data) was obtained from the MS peak of the fragment ion of the thioacidolysis degradation product (molecular formula: $\rm C_{13}H_{21}O_2SiS$) shown in Figure S9 to calculate the ^{13}C labeling ratio. The ^{13}C existence probability at the ring-1 position was calculated using the relative frequency as follows: First, two sets of m/z 269–277 isotopic distributions for the compound of natural abundance (calc-data) and the ring-1- ^{13}C compound (calc-data) were calculated. The exp-data was interpreted as the sum of these two calc-data. Next, the exp-data was fitted by Microsoft Excel (ver. 2307) solver function using the two calc-data to obtain the ring-1- ^{13}C labeling ratio. This procedure evaluated the average ^{13}C ratio of the Ctrl-1,2,3 and NL-1,2,3 samples as 1.11 and 1.07 % (Table S1), respectively. These values are nearly equal to the natural abundance of ^{13}C , 1.07 %.

2.12 Sample preparation for NMR

The enzymatically saccharified lignin (EL) samples were prepared, referring to the previously reported method (Kim et al. 2017). The milled sample (1.0 g) was further treated using a planetary ball mill (PUL-VERISETTE 6 classic line, FRITSCH GmbH) with zirconia balls (5-mm diameter, 100 g) in a 45 mL zirconia jar at 600 rpm for 6 h (grinding for 2 min, waiting for 2 min, 180 cycles) to obtain a ball-milled sample. Thus, the obtained 0.7-g ball-milled sample was suspended in 17.5 mL acetic acid buffer (pH 5.0) in a flask with baffles, and 35-mg cellulysin (CEL-LULYSIN® Cellulase, *Trichoderma viride*, Affiliate of Merck KGaA Darmstadt, Germany) was added into the flask. After shaking for 48 h at 35 °C with light shielding, the mixture was centrifuged, and 35 mg cellulysin and 17.5-mL buffer were added again. This enzymatic treatment was repeated 3 times (48 \times 3 h). The sample was centrifuged and washed with distilled water 3 times and freeze-dried.

The EL sample was acetylated, referring to a previously reported method (Lu and Ralph 2003) to obtain the acetylated EL (ELAc) sample. EL sample (100 mg), 2.0 mL dimethyl sulfoxide (DMSO) (dehydrated by molecular sieves), and 1.0 mL N-methylimidazole (dehydrated by molecular sieves) were mixed in a flask under N_2 atmosphere at 25 °C. After 3 h, 0.6 mL acetic anhydride was added into the flask and stirred for 24 h at 25 °C with a light-shielding. The solution was dropped into ice water to stop the reaction. The precipitated sample was washed with distilled water 3 times and freeze-dried.

2.13 Liquid-state NMR measurements

Liquid-state 2D HSQC, 2D HMBC, and quantitative ¹³C (an inverse gated decoupling mode) NMR measurements were conducted using Bruker Avance 600 spectrometer equipped with a cryoprobe

(Bruker BioSpin GmbH, Rheinstetten). The EL samples were soluble in DMSO- d_6 , and the ELAc samples were soluble in CDCl₃. The 2D NMR measurement conditions were as follows: resonance frequencies, ¹H 600 MHz and ¹³C 150 MHz; sample concentration, 100 mg/mL; solvent, CDCl₃; scan number, 24; temperature, 300 K; data points, 2048 \times 256; spectral width of F1 –1 to 11 ppm \times F2 7.5– 184.5 ppm; acquisition time, 0.142 s; pulse delay, 1.2s. For HSOC, Bruker pulse program, hsqcedetgpsp.3; J, 145 Hz; measurement time, 10.2 h. HSQC processing parameters: data points, 2048 × 1024; window function, QSINE (F1: LB 0.3, GB 0.1, SSB 2, TM1 0.1, TM2 0.9. F2: 1.00, GB 0, SSB 2, TM1 0, TM2 0). For HMBC, Bruker pulse program, hmbcgplpndqf; long-range J, 15 Hz; measurement time, 12.4 h. HMBC processing parameters: data points, 1024 × 1024; window function SINE (F1 and F2: LB 0, GB 0, SSB 0, TM1 0, TM2 0). The cross-peak volume was integrated using the integral function of Topspin software (Bruker, ver. 4.3.0).

The quantitative ¹³C measurement conditions were as follows: sample concentration, 60 mg/mL for EL and 100 mg/mL for ELAc; solvent, DMSO-d₆ for EL and CDCl₃ for ELAc; both solvents contain 0.1 M Cr(III) acetylacetonate as a relaxation reagent (Gansow et al. 1972; Rokhin et al. 1994; Xia et al. 2001); scan number, 30,000 for EL and 25,000 for ELAc; acquisition time, 1.4 s; pulse delay, 1.7 s; temperature, 300 K.

2.14 Solid-state ¹³C CP/MAS NMR measurements

Solid-state ¹³C CP/MAS NMR measurements were carried out on a Bruker AVANCE NEO 500 spectrometer. The measurement conditions were as follows: resonance frequencies, ¹³C 125 MHz; MAS, 13.75 kHz; acquisition time, 40.96 ms; contact time, 2.0 ms; relaxation delay, 3.0 s; scan number 15,000; temperature, 300 K. The spinning side bands should be 110 ppm (= 13.75 kHz/125 MHz) from the original signals. The lowest-field signal in the solid-state ¹³C NMR spectrum of EL was at 155 ppm; therefore, the region 50-155 ppm should not be overlapped with the spinning sidebands. The measured EL sample was the same one for solution-state NMR.

2.15 NMR data processing for difference 1D spectra

The obtained ¹³C NMR spectra were exported to ASCII data by Bruker Topspin software (ver. 4.2.0, Bruker BioSpin GmbH, Rheinstetten). After normalization, the not-labeled spectrum was subtracted from the ring-1 labeled spectrum using the methoxy carbon signal for solution-state data or the aromatic carbon signals at 151 ppm for solid-state data. The subtraction and the peak area integrations were done using Microsoft Excel (ver. 2307). The nonlabeling sample data obtained for the NL-2 sample was used for the processing.

3 Results and discussion

3.1 Synthesis of [ring-1-13C]coniferin

The synthesis of [ring-1-13C]coniferin has been reported by Terashima and Parkås (Parkås et al. 2004; Terashima et al. 2003). It was synthesized by the reaction of triformyl[13C] methane (13CH(CHO)₃) with methoxyacetone in an alkaline solution to yield [ring-1-13C] vanillin, followed by the addition of the side chain and glucose to obtain [ring-1-13C]coniferin (Terashima et al. 1996). However, the yield of $[1-^{13}C]$ vanillin was low at 9 % in their papers. In this study, a new method was presented for obtaining [ring-1-13C] vanillin by applying the reaction of $[2^{-13}C]$ diethyl malonate with 4H-pyran-4-one (Beyer et al. 1998; Lang et al. 2002; Marshall et al. 2009) to yield ethyl [ring-1-13C]benzoate, followed by reduction and introduction of a methoxy group. The yield from [2-13C] diethyl malonate to [ring-1-13C]vanillin was 17 %, about double that of the previous procedure. The total yield from [2-13C]diethyl malonate to [ring-1-13C]coniferin was 6.7 %.

3.2 Incorporation of [ring-1-13C]coniferin to xvlem of G. biloba

Previous studies have shown that by growing ginkgo for approximately one month in tap water after coniferin administration, the administered coniferin is incorporated into the lignin at a position slightly distant from the cambial zone (Xie and Terashima 1991). Therefore, five layers of the newly formed xylem were peeled from the cambial zone with a thickness of approximately 200 μm, measuring the ¹³C labeling ratio of each layer, and selecting the layer with the high ¹³C labeling ratio as the sample for analysis.

The ¹³C labeling ratio of each layer of L-1, L-2, and L-3 samples was evaluated and is shown in Table 1. The layer of the newly formed xylem, approximately 400-600 µm from the cambial zone, had a relatively high ¹³C labeling ratio and was used as the sample for NMR analysis. Significantly, the L-3 sample had the highest labeling ratio. From these results, the third and fourth layers of the L-3 sample were used as EL (solid-state ¹³C CP/MAS and solution-state quantitative ¹³C

Table 1: ¹³C ratio at ring-1 of lignin of the newly formed xylem layer samples in the [ring-1-¹³C]coniferin administrated *G. biloba* shoots.

Sample layer distance from the cambial zone	1	2	3	4	5
	0–200 µm	200–400 μm	400–600 μm	600–800 μm	800–1000 μm
r-1- ¹³ C ratio of L-1	1.35 %	1.07 %	3.89 %	3.87 %	2.16 %
r-1- ¹³ C ratio of L-2	1.07 %	1.90 %	2.58 %	2.18 %	2.88 %
r-1- ¹³ C ratio of L-3	1.98 %	4.50 %	8.36 %	4.41 %	3.52 %

measurements) and ELAc (solution-state 2D and quantitative ¹³C measurements), respectively.

3.3 Spirodienone ring-1 signals in liquidstate 2D NMR spectra

ELAc of the labeled sample was subjected to HSQC measurements to confirm the β -1 structure. The results for aliphatic and aromatic regions are shown in Figures 3 and S10, respectively. The HSQC spectrum was obtained by a multiplicity-edited experiment, and CH₂ was colored differently from CH and CH₃. Considering the previously reported spirodienone signals (Zhang et al. 2006), cross signals at 81.37/5.14 and 56.63/2.96 ppm were assigned as the C α '-H and C β '-H of the spirodienone structure, respectively. No specific cross signals were confirmed for 1,2-diarylpropane (Ralph et al. 2009) or isochroman (Peng et al. 1999) structures.

The HSQC C α -H cross-peak volume is a widely accepted method for their relative amount evaluation. In Figure 3, β -O-4, β -5, β - β , dibenzodioxocin (DBDO), and β -1 (C α '-H) signals were evaluated as the relative amount to G2-H signal and summarized in Table 2. Here, the amount of β - β should be half as the dimer mol. The amount of β -1 was the smallest among these 5 types. Further examination for the β -1 quantification will be conducted later using 1D 13 C spectra.

The ring-1 carbon of the spirodienone B-ring is a quaternary carbon and cannot be observed by ¹H ¹³C HSQC. Therefore, the carbon signal was further investigated by ¹H ¹³C long-range correlation (HMBC) measurements. The

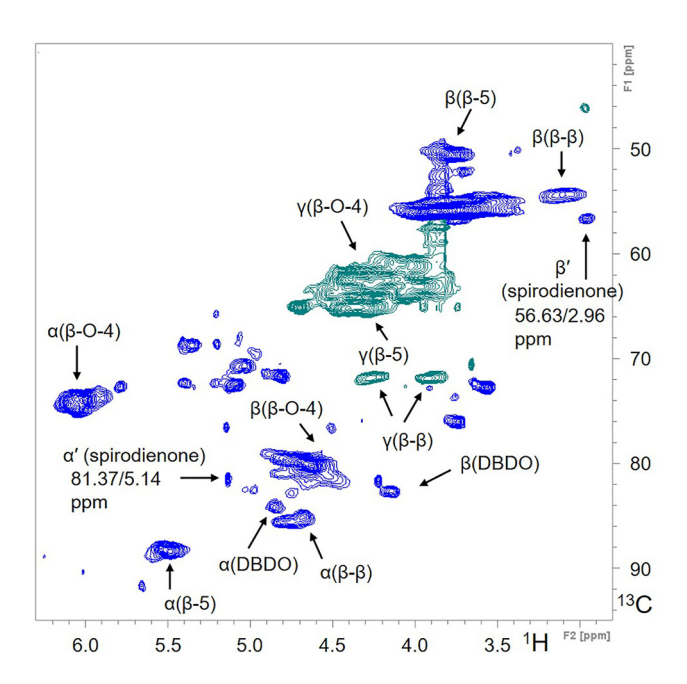


Figure 3: ¹H-¹³C HSQC NMR spectrum of L3-4 ELAc in CDCl₃.

Table 2: Relative amount of bonding patterns, evaluated by HSQC cross-peak volumes.

Unit	Amount
β-0-4	0.481
β-O-4 β-5	0.176
β-β	0.098
β-1	0.023
DBDO	0.033

remote couplings from the hydrogens at ring-2, 5, and 6 positions to the ring-1 carbon were detected (Figure S11). Accordingly, the ring-1 carbon of the spirodienone B ring was assigned to the signal at 54.73 ppm. The ring-1 signal was very close to the methoxy carbon, generally present at 56 ppm, but as discussed below, the two signals could be separated and identified.

3.4 Quantification of spirodienone structures in EL and ELAc samples

A quantitative ¹³C measurement was performed to quantify the spirodienone structure in lignin. The spectra obtained for ELAc are shown in Figure 4. Figure 4a–d shows the spectra of the non-labeling (NL-2) and labeled (L3-4) ELAc samples, respectively. The unlabeled and labeled samples show 110–155 ppm peaks derived from the aromatic carbons. In the labeled sample (Figure 4c), the signal is enhanced in the 120–140 ppm region.

As the methoxy and the spirodienone ring-1 carbons were separated, a difference spectrum was generated by subtracting the not-labeled spectrum from the labeled spectrum after normalization using the methoxy carbon signal. The resulting difference spectrum is shown in Figure 4e and f.

Signals from the aromatic ring-1 carbons were observed in the 120–140 ppm range, and a peak of the spirodienone ring-1 carbon was detected at about 55 ppm. The enlarged spectrum around 55 ppm is shown in Figure 4f. The peak top of the spirodienone ring-1 carbon was 54.72 ppm. This result is in close agreement with the HMBC result above.

By quantifying only the signal derived from the ring-1 carbon in the difference spectrum (Figure 4f), the ratio of the spirodienone structure to the total lignin could be evaluated. The ratio of the peak areas was calculated and obtained a result of 0.72 %. This value is smaller than that evaluated using HSQC volume values.

The spectra obtained for EL are shown in Figure 5. Figure 5a–d shows the spectra of the non-labeling (NL-2) and

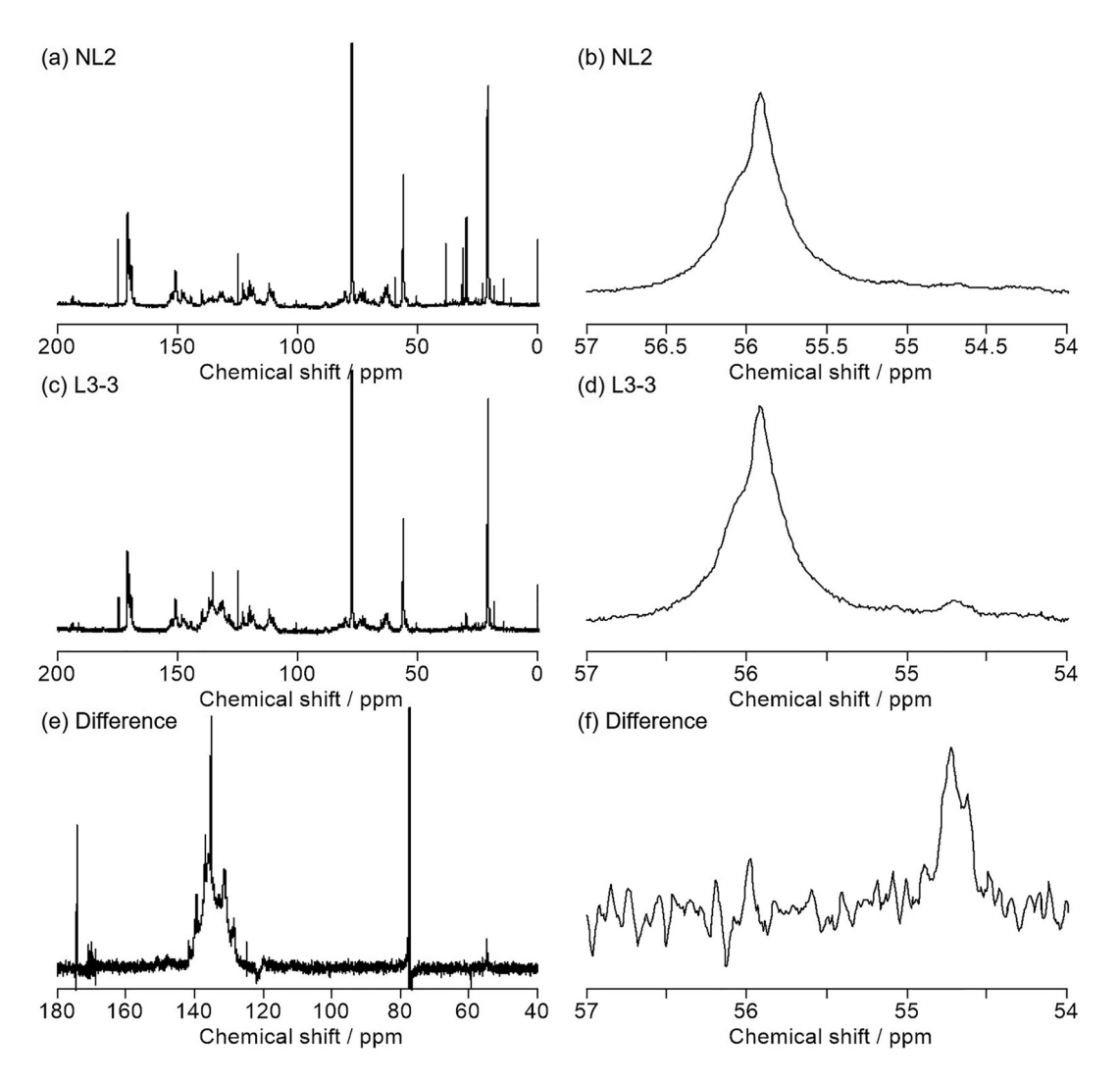


Figure 4: Solution-state quantitative ¹³C NMR spectra of (a, b) NL-2 ELAc, (c, d) L3-4 ELAc, and (e, f) the difference between L3-4 and NL-2 samples.

labeled (L3-3) EL samples, respectively. As in the case of ELAc, peaks derived from the aromatic carbons are found in the range of 110–155 ppm, and in the labeled sample (Figure 5c and d), an enhanced peak due to ¹³C labeling is detected in the range of 120–140 ppm. As the methoxy and the spirodienone ring-1 carbons could also be separated, a difference spectrum was generated similarly. The difference spectrum obtained is shown in Figure 5e and f.

Peaks originating from the aromatic ring-1 carbons were observed around 120–140 ppm, and a peak from the spirodienone ring-1 carbon was found at about 55 ppm. In the enlarged view around 55 ppm shown in Figure 5f, the signal derived from the spirodienone ring-1 carbon was at 54.70 ppm. This value agrees with the result obtained for ELAc. In the same way, the percentage of the peak area of the spirodienone structure was calculated, and the result was

0.68 %. These results indicate that the amount of spirodienone structure is consistent with or without acetylation.

3.5 Solid-state difference spectrum to assign the spirodienone ring-1 carbon

NMR signal positions are often different between solid- and liquid-state measurements. In addition, solid-state NMR signals for amorphous polymers such as lignin are generally broad, making it difficult to assign a clear and independent signal to a substructure. In this study, the detection of the spirodienone ring-1 carbons by solid-state NMR using selective labeling and difference spectroscopy was attempted.

The obtained solid-state ¹³C CP/MAS NMR spectra are shown in Figure 6. Figure 6a and b shows the spectra of the

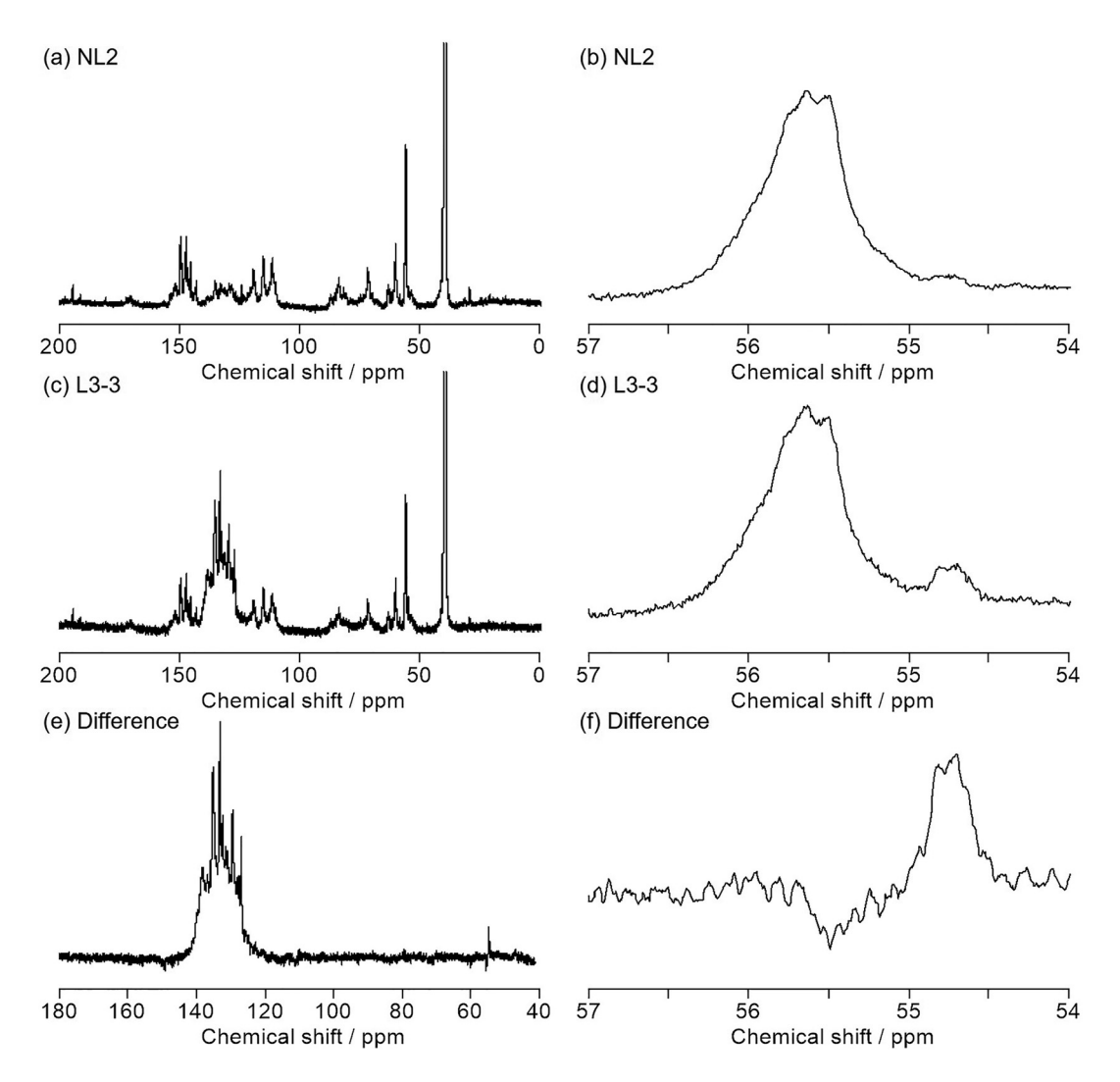


Figure 5: Solution-state quantitative ¹³C NMR spectra of (a, b) NL-2 EL, (c, d) L3-3 EL, and (e, f) the difference between L3-3 and NL-2 samples.

not-labeled sample, and Figure 6c and d shows the spectra of the labeled sample. A methoxy carbon peak was observed at around 56 ppm, and polysaccharide-derived peaks were found between 60 and 110 ppm. Broad peaks derived from aromatic carbons were observed in the range of 110–155 ppm, and in the labeled sample, the peak was enhanced at 134 ppm due to ¹³C labeling.

The peak derived from the spirodienone ring-1 carbon is expected to be close to that of the methoxy carbon. In contrast to the case of liquid-state NMR, their signals could not be separated. Therefore, a difference spectrum was prepared by normalizing the spectra to eliminate the signal from the aromatic carbons connecting to oxygen at about 151 ppm (Aoki et al. 2019; Miyata et al. 2023).

The resulting difference spectrum is shown in Figure 6e and f. A broad singlet peak originating from the aromatic ring-1 carbons was observed at about 134 ppm. This result

can be interpreted as a broadening of the liquid NMR result. Furthermore, this result may suggest that the signal from the ring-1 carbons can be fitted by a single Gaussian peak when peak fitting is performed on the aromatic carbon region in solid-state NMR. Negative difference signals are weakly detected at 60–80 ppm. These negative signals may be derived from polysaccharides because the enzymatic saccharification process between the samples was not fully completed.

A difference signal is positively detected around 56 ppm. An enlarged view of around 56 ppm is shown in Figure 6f. Assuming the methoxy carbon signal in the difference spectrum has been eliminated, this positive signal at 56.11 ppm can be derived from the spirodienone structure. In contrast to the liquid NMR results, the ring-1 peak appeared at a lower magnetic field than the methoxy group. Further experiments should confirm this result.

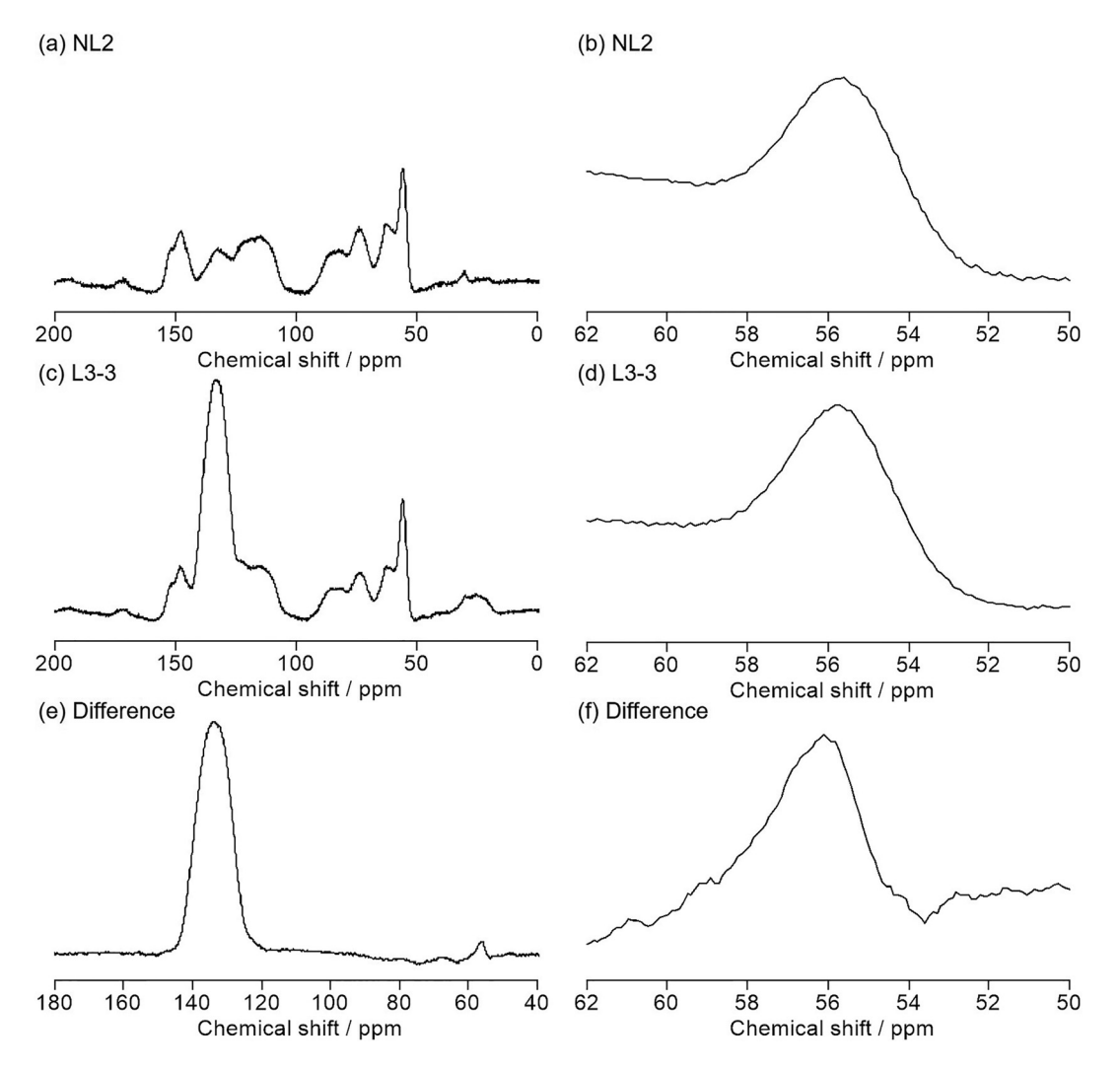


Figure 6: Solid-state 13C CP/MAS NMR spectra of (a, b) NL-2 EL, (c, d) L3-3 EL, and (e, f) the difference between L3-3 and NL-2 samples.

Although the CP/MAS measurement is not quantitative, the ratio of the peak area of the spirodienone ring-1 carbon to the total peak area derived from the aromatic ring-1 carbons was calculated to be 0.91%. This tentative value is not so far from the quantitative value obtained by liquid-state NMR measurements.

4 Conclusions

In this study, [ring-1-¹³C]coniferin was synthesized and administered to *G. biloba* shoots to obtain selectively labeled lignin at the ring-1 position in the *G. biloba* xylem sample. The [ring-1-¹³C]coniferin uptake was evaluated by GCMS analysis, which showed that in ginkgo shoot samples, the labeled coniferin was incorporated at several hundred micrometers distant from the cambial zone, i.e., in the region of

cell wall lignification. The resulting xylem samples were subjected to milling, enzymatic saccharification, and acetylation to prepare samples for liquid- and solid-state NMR. Solution-state NMR detected the spirodienone structure by two-dimensional NMR measurements, and quantitative $^{13}\mathrm{C}$ difference spectra and HSQC showed that the spirodienone structure was present in about 0.7 % of the lignin and 2.3 % to G2-H, respectively.

Acknowledgments: The authors thank K. Koga, M. Kano, M. Torii, and I. Hayashi, Technical Centre of Nagoya University, for helping NMR measurements. They also thank I. Ito for supporting the synthesis of [ring-1-13C]coniferin.

Research ethics: Not applicable.

Author contributions: YM, DA, KF, and MK conceived the research. MH and YM synthesized chemical compounds, and administered coniferin to plant samples. SI, MH, YM, and DA

conducted NMR measurements. SI, YM, and DA wrote the manuscript. All authors read and contributed to the manuscript. **Competing interests:** The authors state no conflict of interest. **Research funding:** This work was supported by ISPS KAKENHI Grant Numbers 18H03959, 19K06168, 23H02274, 23H02275, and the Joint Usage/Research Program on Zero-Emission Energy Research, Institute of Advanced Energy, Kvoto University ZE2022A-20.

Data availability: The raw data can be obtained on request from the corresponding author.

References

- Ämmälahti, E., Brunow, G., Bardet, M., Robert, D., and Kilpeläinen, I. (1998). Identification of side-chain structures in a poplar lignin using threedimensional HMQC-HOHAHA NMR spectroscopy. J. Agric. Food Chem. 46: 5113-5117.
- Aoki, D., Nomura, K., Hashiura, M., Imamura, Y., Miyata, S., Terashima, N., Matsushita, Y., Nishimura, H., Watanabe, T., Katahira, M., et al. (2019). Evaluation of ring-5 structures of quaiacyl lignin in Ginkgo biloba L. using solid- and liquid-state ¹³C NMR difference spectroscopy. Holzforschung 73: 1083-1092.
- Beyer, J., Lang-Fugmann, S., Muhlbauer, A., and Steglich, W. (1998). A convenient synthesis of 4-hydroxy[1-13C]benzoic acid and related ringlabelled phenolic compounds. Synthesis 7: 1047-1051.
- Brunow, G., Ämmälahti, E., Niemi, T., Sipilä, J., Simola, L.K., and Kilpeläinen, I. (1998). Labeling of a lignin from suspension cultures of Picea abies. Phytochemistry 47: 1495-1500.
- Capanema, E.A., Balakshin, M.Y., and Kadla, J.F. (2005). Quantitative characterization of a hardwood milled wood lignin by nuclear magnetic resonance spectroscopy. J. Agric. Food Chem. 53: 9636-9649.
- del Río, J.C., Rencoret, J., Margues, G., Li, J., Gellerstedt, G., Jiménez-Barbero, J., Martínez, Á.T., and Gutiérrez, A. (2009). Structural characterisation of the lignin from jute (Corchorus capsularis) fibers. J. Agric. Food Chem. 57: 10271-10281.
- del Río, J.C., Rencoret, J., Gutiérrez, A., Nieto, L., Jiménez-Barbero, J., and Martínez, Á.T. (2011). Structural characterisation of guaiacyl-rich lignins in flax (Linum usitatissimum) fibers and shives. J. Agric. Food Chem. 59: 11088-11099.
- Ede, R.M., Brunow, G., Simola, L.K., and Lemmetyinen, J. (1990). Twodimensional ¹H-¹H chemical shift correlation and *J*-resolved NMR studies on isolated and synthetic lignins. Holzforschung 44: 95-101.
- Ede, R.M., Ralph, J., Torr, K.M., and Dawson, B.S.W. (1996). A 2D NMR investigation of the heterogeneity of distribution of diarylpropane structures in extracted Pinus radiata lignins. Holzforschung 50: 161-164
- Gansow, O.A., Burke, A.R., and Vernon, W.D. (1972). Temperaturedependent carbon-13 nuclear magnetic resonance spectra of the h^5 cyclopentadienyliron dicarbonyl dimer, an application of a shiftless relaxation reagent. J. Am. Chem. Soc. 94: 2550-2552.
- Habu, N., Matsumoto, Y., Ishizu, A., and Nakano, J. (1990). The role of the diarylpropane structure as a minor constituent in spruce lignin. Holzforschung 44: 67-71.
- Higuchi, T. (1990). Lignin biochemistry: biosynthesis and biodegradation. Wood Sci. Technol. 24: 23-63.

- Kim, H., Padmakshan, D., Li, Y., Rencoret, J., Hatfield, R.D., and Ralph, J. (2017). Characterization and elimination of undesirable protein residues in plant cell wall materials for enhancing lignin analysis by solution-state nuclear magnetic resonance spectroscopy. Biomacromolecules 18: 4184-4195.
- Lang, M., Lang-Fugmann, S., and Steglich, W. (2002). 4-hydroxy[1-13C] benzoic acid. Org. Synth. 78: 113-122.
- Lapierre, C., Monties, B., Rolando, C., and de Chirale, L. (1985). Thioacidolysis of lignin: comparison with acidolysis. J. Wood Chem. Technol. 5: 277–292.
- Lapierre, C., Monties, B., and Rolando, C. (1986). Preparative thioacidolysis of spruce lignin: isolation and identification of main monomeric products. Holzforschung 40: 47-50.
- Lu, F. and Ralph, J. (2003). Non-degradative dissolution and acetylation of ball-milled plant cell walls: high-resolution solution-state NMR. Plant J. 35: 535-544.
- Lundquist, K. (1987). On the occurrence of β-1 structures in lignins. J. Wood Chem. Technol. 7: 179-185.
- Lundquist, K. and Mikshe, G.E. (1965). Nachweis eines neuen Verknupfungsprinzips von Guajacylpropaneinheiten in Fichtenlignin. Tetrahedron Lett. 25: 2131-2136.
- Marshall, L.J., Cable, K.M., and Botting, N.P. (2009). First synthesis of [1,3,5-13C3]gallic acid. *Org. Biomol. Chem.* 7: 785–788.
- Matsumoto, Y., Ishizu, A., and Nakano, J. (1984). Determination of glyceradehyde-2-aryl ether type structure in lignin by the use of ozonolysis. Mokuzai Gakkaishi 30: 74-78.
- Miyata, S., Aoki, D., Matsushita, Y., Takeuchi, M., and Fukushima, K. (2023). Evaluation of guaiacyl lignin aromatic structures using 13CO2 administered Ginkgo biloba L. xylem by quantitative solid- and liquidstate ¹³C NMR. Holzforschung 77: 230-239.
- Parkås, J., Paulsson, M., Terashima, N., Westermark, U., and Ralph, S.A. (2004). Light-induced yellowing of selectively ¹³C-enriched dehydrogenation polymers (DHPs). Part 2. NMR assignments and photoyellowing of aromatic ring-1-3-4-and 5-13C DHPs Nord. Pulp Paper Res. J. 1: 44-52.
- Peng, J., Lu, F., and Ralph, J. (1999). Isochroman lignin trimers from DFRC-degraded Pinus taeda. Phytochemistry 50: 659-666.
- Ralph, J., Lundquist, K., Brunow, G., Lu, F., Kim, H., Schatz, P.F., Marita, J.M., Hatfield, R.D., Ralph, S.A., Christensen, J.H., et al. (2004). Lignins: natural polymers from oxidative coupling of 4-hydroxyphenylpropanoids. Phytochem. Rev. 3: 29-60.
- Ralph, S., Ralph, J., and Landucci, L.L. (2009). NMR database of lignin and cell wall model compounds, Available at: https://www.glbrc.org/ databases and software/nmrdatabase/ (Accessed Sep 20, 2023).
- Ralph, J., Lapierre, C., and Boerjan, W. (2019). Lignin structure and its engineering. Curr. Opin. Biotechnol. 56: 240-249.
- Rencoret, J., Marques, G., Gutiérrez, A., Ibarra, D., Li, J., Gellerstedt, G., Santos, J.I., Jiménez-Barbero, J., Martínez, Á.T., and del Río, J.C. (2008). Structural characterization of milled wood lignins from different eucalypt species. Holzforschung 62: 514-526.
- Rencoret, J., Gutiérrez, A., Nieto, L., Jiménez-Barbero, J., Faulds, C.B., Kim, H., Ralph, J., Martínez, Á.T., and del Río, J.C. (2011). Lignin composition and structure in young versus adult Eucalyptus globulus plants. Plant *Physiol*. 155: 667–682.
- Rokhin, A.V., Kanitskaya, L.V., Kushnarev, D.F., Kalabin, G.A., Smirnova, L.S., Abduazimov, Kh.A., and Pulatov, B.Kh. (1994). Quantitative ¹H and ¹³C NMR spectroscopies of cottonplant dioxane lignin. Chem. Nat. Comp. 30: 745-753.
- Setälä, H., Pajunen, A., Rummakko, P., Sipilä, J., and Brunow, G. (1999). A novel type of spiro compound formed by oxidative cross coupling of

- methyl sinapate with a syringyl lignin model compound. A model system for the β-1 pathway in lignin biosynthesis. J. Chem. Soc., Perkin Trans. 1 1999: 461-464.
- Shimizu, K., Matsushita, Y., Aoki, D., Mitsuda, H., and Fukushima, F. (2021). Reactivity of a benzylic lignin-carbohydrate model compound during enzymatic dehydrogenative polymerisation of coniferyl alcohol. Holzforschung 75: 773-777.
- Terashima, N., Ralph, S.A., and Landucci, L.L. (1996). New facile synthesis of monolignol glucosides, p-glucocoumaryl alcohol, coniferyl alcohol, and syringin. Holzforschung 50: 151-155.
- Terashima, N., Hafrén, J., Westermark, U., and VanderHart, D.L. (2002). Nondestructive analysis of lignin structure by NMR spectroscopy of specifically ¹³C-enriched lignins. Part 1. Solid state study of ginkgo wood. Holzforschung 56: 43-50.
- Terashima, N., Evtuquin, D., Neto, C.P., Parkås, J., Paulsson, M., Westermark, U., Ralph, S., and Ralph, J. (2003). An improved ¹³C-tracer method for the study of lignin structure and reactions - differential

- ¹³C-NMR. In: *Proceedings of 12th international symposium on wood and* pulping chemistry, Madison, Wisconsin USA, pp. 175-178.
- Xia, Z., Akim, L.G., and Argyropoulos, D.S. (2001). Quantitative ^{13}C NMR analysis of lignins with internal standards. J. Agric. Food Chem. 49: 3573-3578.
- Xie, Y. and Terashima, N. (1991). Selective carbon 13-enrichment of side chain carbons of ginkgo lignin traced by carbon 13 nuclear magnetic resonance. Mokuzai Gakkaishi 37: 935-941.
- Zhang, L. and Gellerstedt, G. (2001). NMR observation of a new lignin structure, a spiro-dienone. Chem. Commun. 24: 2744-2745.
- Zhang, L., Gellerstedt, G., Ralph, J., and Lu, F. (2006). NMR studies on the occurrence of spirodienone structures in lignins. J. Wood Chem. Technol. 26: 65-79.

Supplementary Material: This article contains supplementary material (https://doi.org/10.1515/hf-2023-0100).